Topical application of superoxide dismutase mediated by HIV-TAT peptide attenuates UVB-induced damages in human skin

Topical application of superoxide dismutase mediated by HIV-TAT peptide attenuates UVB-induced damages in human skin

Xiaochao Chen, Shutao Liu, Pingfan Rao, Jeremy Bradshaw, Richard Weller

PII: S0939-6411(16)30342-3
DOI: http://dx.doi.org/10.1016/j.ejpb.2016.07.023
Reference: EJPB 12261

To appear in: *European Journal of Pharmaceutics and Biopharmaceutics*

Received Date: 24 March 2016
Revised Date: 15 July 2016
Accepted Date: 22 July 2016

Please cite this article as: X. Chen, S. Liu, P. Rao, J. Bradshaw, R. Weller, Topical application of superoxide dismutase mediated by HIV-TAT peptide attenuates UVB-induced damages in human skin, *European Journal of Pharmaceutics and Biopharmaceutics* (2016), doi: http://dx.doi.org/10.1016/j.ejpb.2016.07.023

Topical application of superoxide dismutase mediated by HIV-TAT peptide attenuates UVB-induced damages in human skin

Xiaochao Chen[1,2], Shutao Liu[1], Pingfan Rao[1], Jeremy Bradshaw[3] and Richard Weller[2,*]

1. College of Biological Science and Biotechnology, Fuzhou University, 2 Xue Yuan Road, University Town 350116, Fuzhou, Fujian, People's Republic of China

2. The University of Edinburgh, Medical Research Council Centre for Inflammation Research, Queens Medical Research Institute, 47 Little France Crescent, Edinburgh, EH16 4TJ, United Kingdom.

3. The University of Edinburgh, Royal (Dick) School of Veterinary Studies, Easter Bush, Roslin, Midlothian, EH25 9RG, United Kingdom.

***Corresponding author:** Dr. Richard Weller (r.weller@ed.ac.uk)

Present address: The University of Edinburgh, Medical Research Council Centre for Inflammation Research, Queens Medical Research Institute, 47 Little France Crescent, Edinburgh, EH16 4TJ, United Kingdom.

Keywords: Ultraviolet; superoxide dismutase; HIV-TAT peptide; erythema; blood flow; sunburn cell; tape stripping; transdermal delivery

Abbreviations: UV, ultraviolet; ROS, reactive oxygen species; SOD, superoxide dismutase; GFP, green fluorescent protein; HIV, human immunodeficiency virus; TAT, transactivator of transcription; CPP, cell penetrating peptide; SC, stratum corneum; MED, minimal erythema dose; SBC, sunburn cell.

Abstract

The purpose of this study was to evaluate whether topical application of superoxide dismutase with cell penetrating peptide (HIV-TAT) could protect against skin damage induced by UVB irradiation in human. The permeability through stratum corneum of large proteins linked to TAT peptide was firstly confirmed by confocal microscopy and tape stripping. Ten healthy volunteers with either Fitzpatrick skin type II or III were recruited in this clinical study. TAT-SOD (300 units/cm^2) and vehicle cream were applied on two symmetric areas of both inner upper arms 1 hour prior to UVB irradiation. After one hour of pretreatment, subjects received 10 incremental doses of UVB on pretreated areas. 24 hours later, erythema, blood flow and apoptotic cells were measured. Pretreatment with TAT-SOD 1 hour prior to UVB radiation promoted a mean minimal erythema dose (MED) increase of 36.6 ± 18.4% (P = 0.013<0.05. n=10) compared to vehicle control. The median blood flow values of all subjects following 2 and 3-MED of UVB were 107.8 ± 51.0 units and 239.5 ± 88.0 units respectively, which accounts for 26 % and 25 % decrease with respect to vehicle groups. These data suggest that TAT-SOD significantly suppresses UVB induced erythema formation and blood flow rise. Furthermore, the pretreatment with TAT-SOD 1 hour prior to 2-MED of UVB irradiation reduced the apoptotic sunburn cell formation by 47.6 ± 8.6 % ($p<0.0001$) in all subjects. Evaluating results generated from all measurements, we conclude that topical application of TAT-SOD significantly attenuates UVB-induced skin damage in man. These biological effects of TAT-SOD are probably

mediated via its free radical scavenging properties, clearly differentiating it from other physical sunscreen agents.

INTRODUCTION

Ultraviolet irradiation in sunlight generates reactive oxygen species (ROS) in skin that can oxidize nucleic acids, proteins and lipids, resulting in acute and chronic skin damage. The acute effects include erythema, tanning, and immune suppression. Long-term adverse effects of UV exposure are photoaging and photocarcinogenesis [1,2]. UVB (280-320nm) makes up around 5% of terrestrial ultraviolet radiation and is generally regarded as the prime cause for direct DNA damage in skin, but also generates reactive oxygen species (ROS), while the substantial amount of ROS generated by UVA (320-400nm) are more responsible for photoaging and photocarcinogenesis [3-5].

To protect against ROS damage, the skin is well equipped with a large network of enzymatic antioxidants, such as superoxide dismutase (SOD) and catalase, and non-enzymatic antioxidants, which function in synergy to neutralize oxidative stress [6]. Numerous studies have shown that the SOD activity is drastically depleted after UV irradiation, leading to oxidative stress and the progression of chronic skin damage [7-10]. Nevertheless, the reduction can be compensated by exogenous supplementation or endogenous up-regulation of SOD, as a result of which keratinocytes are more resistant to oxidative stress induced injury.

Indeed, previous studies have elicited many valuable clues indicating that the up-regulation of SOD level is an effective and promising strategy to combat UV-induced skin damage. Takahashi *et al*. found that the stable transfection of copper-zinc-SOD expression vectors into human keratinocytes could make them more resistant to UVB-induced apoptosis [10]. Decraene *et al*. reported that a SOD mimetic (EUK-134) provided a direct protection against UVB-induced oxidative stress by inhibition of the mitogen-activated protein kinase (MAPK) pathways, resulting in a significant increase in human keratinocytes survival *in vitro* [11]. Furthermore, Murakami *et al*. reported Cu, Zn-SOD deficient mice showed more serious atrophic morphology accompanied by the degeneration of collagen and elastic fibers in skin, which could be also induced by UV irradiation [12].

Taking all of above evidence together, it appears that ROS plays a crucial role in mediating the deleterious effects induced by UV irradiation. The possibility to introduce exogenous SOD, the key intracellular antioxidant enzymes, into keratinocytes would contribute to protection against UV-induced skin damage. In an attempt to augment this naturally photoprotective strategy, topical application of SOD might be a promising one. To accomplish this goal, it is necessary to develop formulations that allow stability of this inherently unstable SOD protein. It is also necessary to develop formulations that allow SOD to penetrate through the stratum corneum (SC) in adequate concentrations, with few side effects.

Transdermal drug therapy is an attractive route of administration because it provides higher patient acceptance and compliance and also avoids the first-pass hepatic metabolism. However, a relative lack of effective methods to deliver active agents efficiently through the relatively impermeable SC has been a major hindrance. Over recent decades, several physical methods, such as electroporation and iontophoresis, have been designed to tackle this poor transdermal efficiency, but the results were disappointing. A recent promising technique to deliver bioactive drugs across the epidermal barrier is the use of cell penetrating peptides (CPPs), including HIV-TAT peptide (^{47}YGRKKRRQRRR^{57}) [13]. Since the first discovery of HIV-TAT peptide, the cell penetrating peptides have been shown to facilitate delivery of a wide variety of biomolecules across cell membrane [14,15]. The potential of this technology resides in the high efficiency and relatively low toxicity of CPPs conjugated to bioactive cargoes. A remaining challenge is to elucidate their exact uptake mechanisms and particularly their transdermal delivery [16].

Accumulating studies are showing that CPPs can successfully enhance the transdermal absorption of therapeutic molecules for the treatment of various skin diseases. Uchida *et al*. reported that the combination of TAT and the tight junction opening AT1002 peptide, effectively accelerated transdermal siRNA delivery in mice and strongly suppressed symptoms of atopic dermatitis. [17]. Furthermore, Kashio *et al*. reported that an artificial antiapoptotic protein, FNK, mediated with TAT peptide could enter the cochlea and effectively attenuate aminoglycoside-induced apoptosis of cochlear sensory hair cells in a guinea pig model [18]. More recently, Ookubo *et al.* used poly-arginine (R11) to enhance transdermal delivery of several tyrosinase inhibitors on a guinea pig model and found the fusion protein efficiently penetrated through the SC and significantly inhibited UV-induced melanin synthesis [19].

Although convincing evidence shows that the successful transdermal delivery of various biomolecules can be mediated by CPPs in animal or *ex vivo* models, no transdermal study related with SOD has been reported so far. Furthermore, no clinical study based on transdermal application of SOD against UV-induced skin damages has yet been investigated. The aim of this study is to evaluate whether pretreatment with stratum corneum permeable TAT-SOD protein could subsequently attenuate UVB-induced skin damage in man.

2. MATERIALS AND METHODS

Chemicals

All reagents used were from Sigma Aldrich unless mentioned. Freeze-dried TAT-SOD recombinant protein (310,000 units/mg protein, purity > 98%) was kindly provided by Institute of Biotechnology,

Fuzhou University, China. The TAT-SOD protein is a 164-residue monomeric form of human Cu/Zn-SOD fused with HIV-TAT peptide (^{47}YGRKKRRQRRR^{57}). Molecular weight of this protein is 17 kDa. Purified GFP and TAT-GFP recombinant protein were also provided by Institute of Biotechnology, Fuzhou University, China. Molecular weights of these two proteins are 26.9 and 28.5 kDa, respectively.

***Ex-vivo* skin permeation of TAT-GFP by confocal microscopy**

To evaluate the skin penetration of wild-type GFP and recombinant TAT-GFP, redundant human skin from patients who had undergone abdominal plastic surgery was used. Great care was taken to maintain the integrity of the skin. The subcutaneous fatty tissue was removed using a scalpel. Skin explants of 20 mm in diameter were punched out, sterilized in 70% alcohol for 10s, rinsed in DMEM culture medium with antibiotics (Gibco, Paisley, England) 3 times and transferred onto a 6-well culture plate. Finally, skin explants were submerged into DMEM culture medium in presence of GFP or TAT-GFP at a final protein concentration of 20 μM, and cultured in the 5% CO^2 incubator at 37℃ for up to 2 hours.

At different endpoints of the penetration experiment (0.5, 1 and 2 hours), 2mm punch biopsies were obtained from the center of skin explants with TAT-GFP or GFP pretreatment. The biopsies were snap frozen using liquid nitrogen, embedded in O.C.T. embedding medium (Tissue-Tek, Pelco International, USA), and sectioned (8 μm, perpendicular to the skin) using a cryostat microtome (Leica, Wetzlar, Germany). The sections were visualized with a confocal microscope (Leica, TCS SP5, German) at a 20X objective, PMT 800 V, and eGFP filter set (ex 488nm / em 592nm).

Skin permeability of TAT-SOD by tape stripping

Five healthy volunteers were recruited in this part of study. 2 mg/cm^2 of two creams were applied on two symmetric areas of their both inner upper arms, one containing TAT-SOD protein at 300 units/cm^2 (150 units SOD/mg cream), the other a vehicle. After 1 hour pretreatment, the test areas were carefully cleaned with ethanol and warm water several times. D-Squame® (CuDerm Corp., Dallas, TX, USA) strips, diameter 22 mm, surface area 3.8 cm^2, were used to sample the SC. Strips were placed on the skin, which was outlined with a permanent pen to ensure sampling from the same site. Equal pressure was applied to each strip by pressing with a spring-loaded stamp for thirty seconds. The comparatively high pressure was a prerequisite for obtaining reproducible amounts of SC. Then the strips were removed with tweezers in a single rapid movement and stored on a cellophane sheet at -80°C for further analysis. The specific SOD activity was evaluated on a series of 20 tape stripping samples collected from each subject (n=5).

Detection of SOD activity on tape strips

The SOD assay was adapted from a well plate method. A D-squame® tape strip was perforated with

a punch and three small pieces (∅=5 mm) were lined at the bottom of a well of an opaque 96-well plate (Corning, Costar, Acton, MA). SOD from bovine erythrocytes was used as an external standard, in which case a blank strip was put in the well. SOD activity was assayed using Sigma SOD assay kit (19160, Sigma, USA) following the manufacturer's instructions. The reaction started immediately when 220 µl of reaction mixture was added to each well. This assay is based on the xanthine/ xanthine oxidase catalytic system. After SOD measurement, the tape strips were removed and stored in an Eppendorf tube for protein analysis. Specific SOD activity was obtained after normalizing to the total protein content on the stripping.

Protein analysis on tape strips

The total amount of protein on the D-squame® tape strip was quantified after acid hydrolysis at elevated temperature. Each removed tape strip was incubated in an Eppendorf tube containing 1.5 ml HCl (6 mol/L) at 120°C for 20 hours for complete hydrolysis. After centrifugation, the supernatant was diluted (1: 20) in 1 mol/L borate buffer pH 9. The total protein content was the determined using a colorimetric Bradford protein assay (Bradford reagent, Bio-Rad Labs., Hercules, CA) according to the microplate working protocol. In the experimental setup, the protein assay was conducted by adding 250 µl of cold Bradford Reagent to 25 µl of sample. After 5 minutes incubation at room temperature, the optical density was measured with a microplate reader at a wavelength of 595 nm (Multiskan EX; Thermo Electron Corporation Vantaa, Finland). The protein content of each removed adhesive tape was analyzed in triplicate (n = 3), and the mean value was used for further evaluation. Three blank adhesive tapes (n = 3) were respectively extracted in exactly the same fashion as the protein-covered tapes, and analyzed with every round of analysis. The mean value of these blank tapes served as the respective control to account for background noise. The total protein amount was always determined on the same strip as the SOD activity analysis occurred.

UVB source

A custom made UVB radiation source by Professor Brian Diffey (Regional Medical Physics Department, Newcastle, UK) was used for the following UV irradiation experiments. This unit consisted of a broadband UVB lamp housed within an enclosed unit, with 10 apertures of 9 mm diameter anterior to the UVB lamp to enable 10 incremental doses (38 to 300 mJ/cm^2) to be delivered simultaneously. All 10 apertures were within an area of 7 cm × 3 cm. The maximum dose aperture did not contain any metal foil filter, while the other 9-dose apertures were backed by perforated metal foil with grids containing holes of differing sizes to allow for the nine increasing doses. The UVB lamp casing was made of UV opaque plastic. The unit also consisted of a digital photodiode that switched the lamp off automatically when appropriate doses at the apertures were delivered. A Philips UVB broadband PL-S 9w/12 (Philips, Eindhoven, Netherlands) lamp with a main emission between 275 and 365 nm and maximum at 313 nm was used as UVB source. All lamps and doses were calibrated to national and European standards.

Clinical protocol

Ten healthy volunteers with either Fitzpatrick skin type II or III were recruited in this part of study. None of the subjects had been exposed to recreational UV radiation or sun beds at least 3 months prior to participation, and were using neither topical nor systemic medication at the time of the study. The age range was 23~30 y (median, 24 y), and there were three males and seven females. The procedures were explained in detail to all subjects. They had provided signed informed consent prior to participation. The clinical study was undertaken in accordance with the Declaration of Helsinki (http://www.wma. net/e/policy/b3.htm) and was given a favorable ethical opinion by the Lothian Regional Ethics Committee (reference number: 10/S1103/38) and the NHS Lothian R&D office (reference number: 2010/R/DER/03). The study was performed at the Department of Dermatology, University of Edinburgh.

Before any treatment, two templates with a 7 cm × 3 cm area were marked on two symmetric areas of both inner upper arms. Each template contained ten irradiated sub-sites and one non-irradiated sub-site. 2 mg/cm^2 of two creams were applied on the skin, one Dermabase® cream (Paddock Laboratories Inc., USA) as a vehicle, the other containing TAT-SOD protein at 300 units/cm^2 (150 units SOD/mg cream). To avoid any disruption and maximize the transdermal absorption, two pretreated areas were covered by Tegaderm® films (3M Health Care, USA). After one hour pretreatment, subjects were instructed to carefully clean the treated areas with ethanol and warm water for several times. Then subjects received 10 incremental doses of UVB on two symmetric areas of both inner upper arms. Irradiances were from 38 to 300 mJ/cm^2 of UVB. 24 hours later, subjects underwent erythema, blood flow and sunburn cells measurement on pretreated areas.

Determination of minimal erythema dose (MED)

For all studies requiring assessment of the MED prior to commencement, subjects attended on day one when they received ten incremental doses of UVB on both inner upper arms. Subjects returned 24 hours later to have their MED read. A subject's MED was defined as the minimal dose producing uniform erythema with clearly defined template margins. A Minolta spectrophotometer CM-2600d (Minolta Co., Ltd, Osaka, Japan) was used to measure skin color according to a 3-dimensional color system (*L*, *a*, and *b* values). The *L* value referred to lightness of skin; the *b* value (blue-yellow axis) was an indicator of pigmentation; the *a* value (red-green axis) was a measure of erythema formation and the Δa value (a value 24 hours after irradiation minus a value before irradiation) was used to measure skin responses to UV irradiation [20]. Each spot was measured in triplicate.

Blood flow measurement

Cutaneous blood flow, measured as red blood cell flux, was used as another index of erythema. 24 hours after UVB challenge, the cutaneous blood flow at each irradiated site and adjacent non-irradiated skin was measured by a laser Doppler perfusion monitor (MoorLAB, Moor Instruments Ltd., Axminster, UK). The perfusion monitor with two satellite units connected to the server allowed flux readings from three laser probes to be recorded simultaneously. The perfusion monitor was linked to a computer and recordings displayed continuously by MoorSoft v1.31 for Windows. During the measurement, the three laser probes were secured to the overlying test sites of the skin using a ring of double sided adhesive tape and data were collected for at least 10 minutes, from which an average flux was calculated.

Full thickness punch biopsy

After MED quantification by colorimetry, four 4 mm punch biopsies were taken from each subject under sterile conditions and local anesthesia (Lidocaine 1% + Adrenaline). One was taken from non-irradiated, vehicle pretreated skin and served as a negative control. A second biopsy was taken from vehicle pretreated skin that had been irradiated with 2 MED of UVB and served as a positive control. A third biopsy was taken from non-irradiated, TAT-SOD pretreated skin. A fourth biopsy was taken from TAT-SOD pretreated skin that had been irradiated with 2 MED of UVB. In all experiments where skin biopsies were taken a 4mm diameter sterile disposable punch biopsy was used (Stiefel® Laboratories, Bucks, UK). Biopsy wounds were closed using 4/0 ethilon sutures (Ethicon, Johnson and Johnson medical Ltd., W Lothian, UK). All full thickness skin punch biopsies were fixed in 4% buffered formaldehyde for 24 hours and embedded in paraffin prior to processing for immunohistochemistry.

Measurement of apoptotic sunburn cells

4 μm paraffin-embedded sections of each skin biopsy were deparaffinized through graded alcohol and routinely stained with hematoxylin and eosin (H&E) to allow quantification of sunburn cells (SBCs). SBCs were identified in the epidermis by their shrunken eosinophilic cytoplasm and condensed nuclei. Sections were examined microscopically by two independent counters in a blinded fashion for specific histopathological alterations, and images were captured using a Hamamatsu CCD camera (C4742095, Hamamatsu, Japan) mounted on a Leica DMR microscope with the Leica application suit (ver. 2.8.1, Leica Microsystems, Solms, Germany). Positive cells were counted in randomly chosen high power fields (20-fold magnification) from the entire 20-mm length of epidermis for each skin section. The results were expressed as the mean number of SBCs per section. Positive cells in hair follicles and in the dermis were not included in the quantitative analysis, and a non-irradiated site was always served as a negative control for each series of experiments.

Statistical analysis

The significance of difference between TAT-SOD and vehicle pretreated groups was analyzed using paired, two-tailed, Student's *t*-test. Differences between data sets were defined as being significant (*, 0.05>p>0.01), highly significant (**, 0.01>p>0.001), or very highly significant (***, p<0.001). Data were analyzed using Excel 2000 software. All data were presented as mean ± SD.

3. RESULTS AND DISCUSSION

UV absorption spectrum of TAT-SOD protein

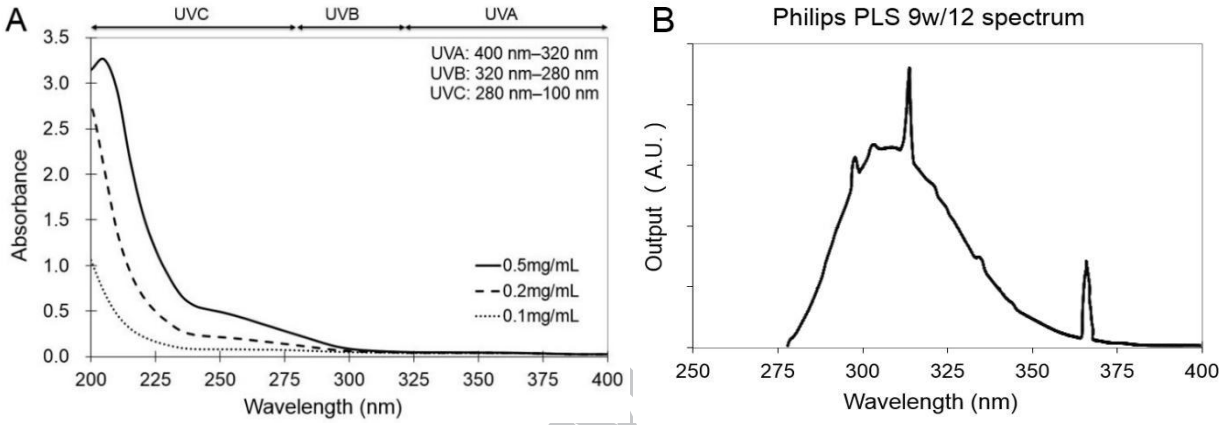

Figure 1: (A). UV absorption spectrum of TAT-SOD protein used in this study. (B). Philips Broadband UVB PL-S 9w/12 lamp spectrum. (Adapted from Philips phototherapy lamps brochure).

As can be observed from the absorbance spectrum of protein, some absorption of UV radiation occurs at shorter (<300nm) wavelengths of UVB. Consideration was therefore given to whether adding a protein to the cream would produce a biologically protective effect against UVB by simple absorption.

To confirm that the protection of TAT-SOD against UVB irradiation was mainly due to the superoxide radical scavenging properties of SOD rather than the physical sunscreen effect of protein itself the UV absorption spectra of TAT-SOD protein at different concentrations was first considered. In the clinical study 2 mg of TAT-SOD cream (150 units SOD/mg cream) was applied per square centimeter of the test area. The concentration of TAT-SOD protein in the cream was $0.5x10^{-3}$ mg/mL which was 200 times lower than the lowest concentration in which the absorption spectrum was measured (0.1 mg/mL). Absorption of UVB at this low level would be undetectable. The broadband UVB source used for the clinical study emits radiation from 275 to 365 nm with a peak at 313 nm, and thus mostly at longer wavelengths than those absorbed by TAT-SOD protein. It is therefore unlikely that any biological effects of TAT-SOD could be caused by a physical sunscreen effect.

Visualization of skin penetration of TAT-GFP by confocal microscopy

To investigate whether TAT peptide could serve as a carrier for transdermal delivery of proteins,

green fluorescent protein (GFP) fused with TAT peptide was used and the skin permeability of GFP and TAT-GFP were tested and compared *ex vivo*. Results examined by confocal microscopy are shown in figure 2. As expected, the treatment of skin with wild-type GFP (20 μM) resulted in fluorescence that was predominantly localized to the surface of SC and no fluorescence was observed in the deeper epidermis and dermis at all time points investigated (figure 2, upper panel). This indicates that wild-type GFP has very poor ability to penetrate the SC layer. Conversely, in TAT-GFP treated skin (20 μM), strong fluorescence was clearly found in the SC layer and weak signals were also observed in the epidermis and dermis at the shortest time of treatment (0.5 hour). When the incubation time increased, the fluorescence in epidermis and dermis region was stronger and deeper (figure 2, lower panel). Strongest fluorescence was found at the incubation period of 2 h. These *ex-vivo* results demonstrate that TAT-GFP was able to penetrate through the SC layer and reach the lower layers of skin. Therefore, we conclude that the skin permeability of TAT-GFP is superior to wild-type GFP and this activity is in a time-dependent manner, which strongly indicate that the topical application system mediated by TAT peptide reported here has high therapeutic potential for the treatment of various skin diseases.

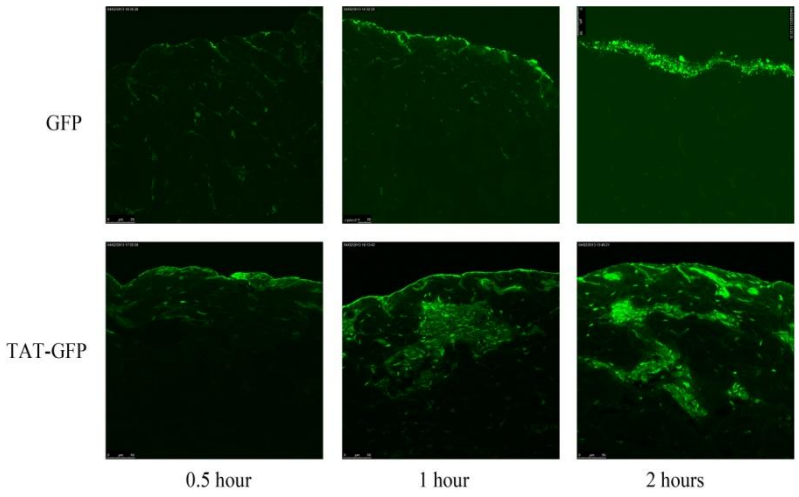

Figure 2. Confocal microscopy of human skin sections with GFP or TAT-GFP treatment under different incubation periods (0.5, 1 and 2 hours). Sections were visualized using eGFP filter through a 20X objective. Scale bars are 50 μm. The experiment was performed in 6 replicates. Upper panel, with GFP treatment; lower panel, with TAT-GFP treatment.

Penetration of TAT-SOD through stratum corneum by tape stripping

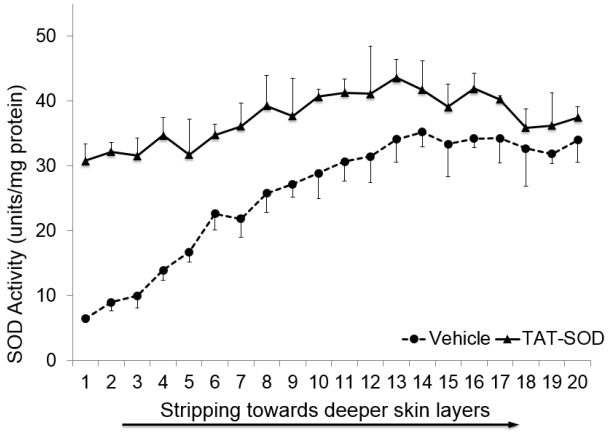

Figure 3: SOD activities on a series of 20 tape strippings from human stratum corneum with TAT-SOD or vehicle pretreatment (n=5). The results are shown as mean ± SD.

Although we have shown that TAT-GFP can efficiently penetrate through the SC layer, no direct evidence on TAT-SOD was gained. As the molecular weight of GFP (26.9 kDa) is larger than that of SOD (17 kDa), it was expected that TAT-SOD could have better penetration in skin. To investigate the skin permeability of TAT-SOD, tape stripping combined with the SOD activity assay was next used. Various *in vivo* methods for measuring transdermal absorption of drugs are available, for example blood withdrawal through a venous cannula, microdialysis, and skin blistering [21]. Recently, tape stripping has been widely used as a fast and comparatively non-invasive technique to measure dermal drug absorption into skin [22,23]. Combined with validated analytical assays for the measurement of bioactive substances, tape stripping has been verified as a superior and reproducible method to approximate transdermal permeability coefficients and partition coefficients in various clinical studies [24,25].

Five volunteers were recruited in this *in vivo* study. As shown in Figure 3, the specific SOD activity was evaluated on a series of 20 tape strip samples collected from each subject using two symmetric areas on both of the inner upper arms. In the vehicle pretreated arm, a linear increase of SOD activity was found in SC from the surface down to deeper layers. A peak value was detected at layer 14 and a plateau was found from layer 14 onward. Such a gradient of SOD activity can be explained by the higher levels of environmental oxidative stress, such as UV radiation and air pollution, that the outer layers of skin are exposed to, with consequent depletion of antioxidant enzyme availability [26].

Due to the high efficiency of translocation mediated by TAT peptide, a significant increase of SOD activity on the TAT-SOD pretreated arm was found from first layer onward when compared to the vehicle pretreated arm. The mean percentage of increase accounted for 250.2% at the first 4 layers and 33.9 % from layer 5 onward. These intriguing data also show that the transdermal delivery of SOD mediated by TAT peptide could efficiently penetrate through the SC, confirming that the topical application system mediated by TAT peptide was effective. Although, the exact mechanism

for transdermal delivery of CPP-linked proteins has not been elucidated, a model of pore formation has been proposed to be a more feasible model for the *in vivo* translocation of large biomolecules, like proteins and liposomes [27].

Suppression of UVB-induced erythema formation by TAT-SOD

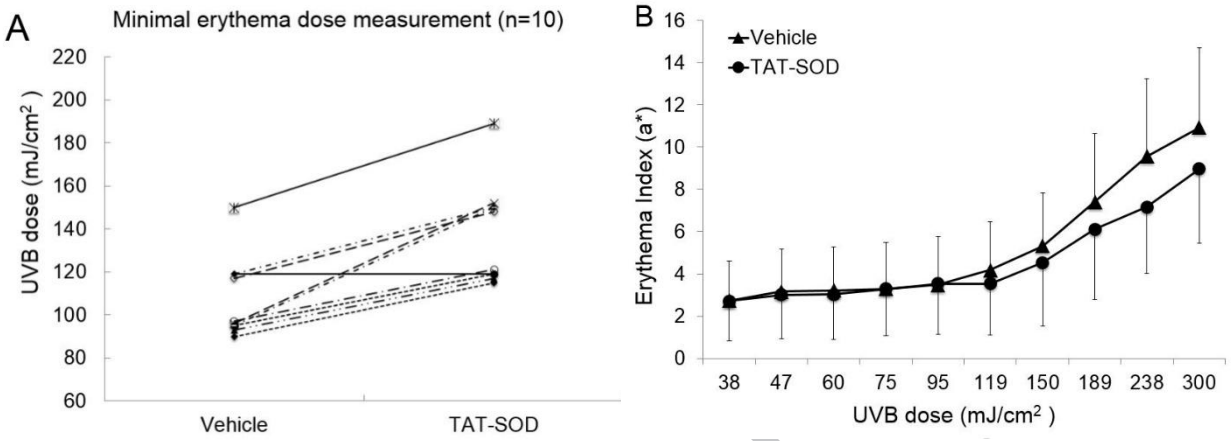

Figure 4: (A). Minimal erythema dose (MED) values at 24 hours after UVB irradiation with vehicle or TAT-SOD pretreatment were measured by colorimetry. A line links value of vehicle and TAT-SOD pretreated skin (300 units/cm^2 of skin area) in a single subject (n=10). The significance of differences (*P*-value) between two pretreated groups was determined by using paired, two-tailed, Student's *t*-test. (B). Erythema response at 24 hours after UVB irradiation with vehicle or TAT-SOD pretreatment (300 units/cm^2 of skin area). Tested areas on both of inner upper arms were irradiated with 10 incremental doses of UVB. The results are shown as mean ± SD (n=10).

To evaluate the potential protective effect of TAT-SOD on UVB-induced skin damage in human skin, three biomarkers were used: erythema, blood flow, and sunburn cell formation. Erythema or sunburn redness is an acute and conspicuous cutaneous inflammatory response that follows excessive exposure to UV radiation, caused by dilation of the blood vessels in dermis [2, 28]. UVB-induced erythema occurs approximately 4 hours after exposure, peaks around 24 hours, and fades over a day or so, in fair-skinned and older people [29,30]. Since erythema is readily visible by non-invasive methods and can be monitored over time, it has been widely used in photo-biological studies. Nevertheless, there have been no published studies looking at the effect of topical application of SOD upon UV-induced erythema formation in man.

Ten healthy volunteers (mean age 24 years; range 23–30) participated in this part of the study. Before any treatment, two templates with a 7 cm × 3 cm area were marked on two symmetric areas of both inner upper arms. Each template contained ten irradiated sub-sites and one non-irradiated sub-site. TAT-SOD cream was applied to the template area on one inner upper arm (300 units/cm^2) and vehicle cream on the other. Two pretreated areas were covered by Tegaderm® films (3M Health Care, USA) to avoid any disruption. One hour later, the TAT-SOD and vehicle pretreated areas were

carefully cleaned and then irradiated with 10 incremental doses of UVB (from 38 to 300 mJ/cm^2). 24 hours after UVB irradiation, MEDs at test areas from ten subjects were measured by colorimetry. Results from ten subjects are shown in Figure 4A. Topical application of TAT-SOD caused a significant increase in MED in 9 of 10 subjects. The rise of MED was highest in two of phototype II subjects, increasing from 95 to 150 mJ/cm^2 (A 58% increase over vehicle), while in other phototype II subjects MED rose from 95 to 119 mJ/cm^2, which means an increment of 25.3%. MED increment in three of phototype III subjects was 26.0% (from 150 to 189 mJ/cm^2 and 119 to 150 mJ/cm^2 respectively) with respect to vehicle. One phototype III subject did show an increase in MED following TAT-SOD pretreatment. The significance of differences (*P*-value) between two pretreated groups was determined by using paired, two-tailed, Student's *t*-test. Thus, the topical application of TAT-SOD cream 1 hour prior to UVB radiation promoted a mean MED increase of 36.6 ± 18.4% ($P = 0.013<0.05$) in 10 subjects, indicating a suppressive effect of TAT-SOD upon UVB induced erythema formation.

The mean erythema readings at 10 incremental UVB doses from all 10 subjects are presented in Figure 4B. No significant erythema response was detected from 38 to 95 mJ/cm^2. However, TAT-SOD provided protection against erythema formation at all irradiance levels above MED when compared with vehicle. The percentage of decrease accounted for 10, 20, 40, and 33% respectively at 150, 189, 238 and 300 mJ/cm^2. In addition, none of subjects irradiated with these doses of UVB (up to 3 MED) developed clinical signs of skin damage, which excluded the possibility that the topical delivery of SOD mediated by HIV-TAT peptide have any adverse effects in skin.

Inhibition of UVB-induced blood flow increment by TAT-SOD

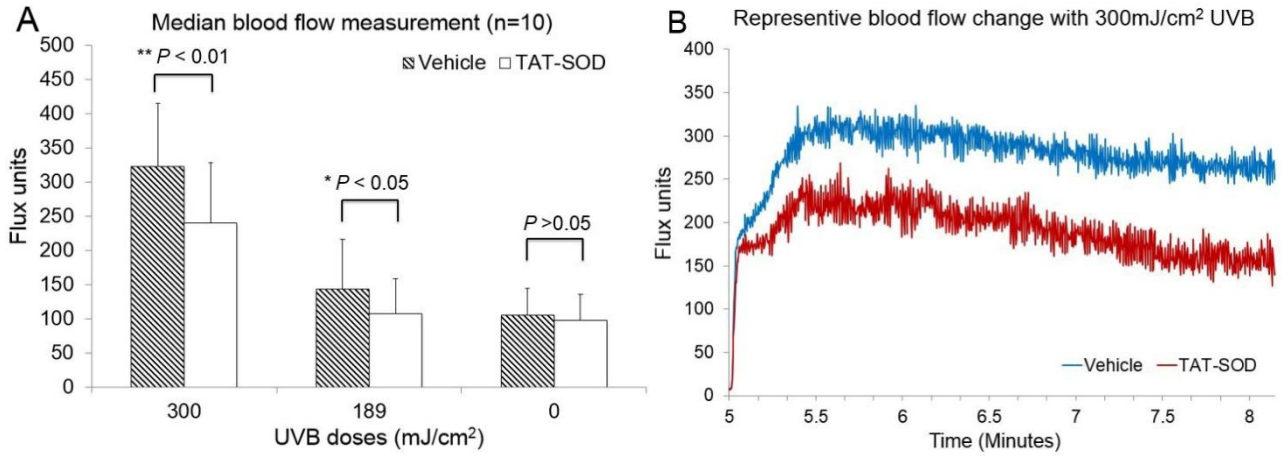

Figure 5: (A). Median blood flow values in vehicle or TAT-SOD pretreated skin (300 units/cm^2 of skin area) were measured at 24 hours after challenge with 2 and 3 MED doses (189 and 300 mJ/cm^2) (n=10). Blood flow values in non-irradiated areas on both of the forearms are shown for comparison (0 mJ/cm^2). The results are shown as mean ± SD. The significance (*P*-value) between vehicle and TAT-SOD groups was determined by using paired, two-tailed, Student's *t*-test. (B). A representative change in blood flow at 24 hours after 300 mJ/cm^2 UVB irradiation with vehicle or TAT-SOD

pretreatment (300 units/cm^2 of skin area). The UVB doses of 300 mJ/cm^2 was selected as equivalent to 3-MED for subject 5.

Next, we used cutaneous blood flow as another index of erythema. It was measured as red blood cell flux using a laser Doppler perfusion monitor. In previous studies, both Andersen and Youn suggested that the blood flow response after UVB irradiation are divided into two phases depending on doses of UVB irradiation [31,32]. The cut-off point between two phases is around MED. At doses lower than MED, the maximal blood flow response was seen after 8 hours, and at doses higher than MED, the maximal response was seen after 24 hours. Furthermore, at higher UVB doses, the resulting increase in blood flow was proportional to UVB dose. In order to yield more clear clues on the potential protective effect of TAT-SOD towards UVB-induced blood flow response, 2 and 3 MED of UVB were used in the following assessments.

Twenty-four hours after UVB challenge, the blood flow of each irradiated and adjacent non-irradiated areas were measured. Median blood flow values after challenge with 2 and 3 MED (189 and 300 mJ/cm^2) are shown in Figure 5A. Vehicle pretreated areas showed highly consistent and significant increases in blood flow. The median blood flow values following 2 and 3 MED increased to 143.6 ± 72.2 units and 322.6 ± 92.7 units respectively, compared to the base line value 105.2 ± 38.6 units. In the meantime, much lower blood flow increments were found in TAT-SOD pretreated areas. The median blood flow rise following 2 and 3 MED were 107.8 ± 51.0 units and 239.5 ± 88.0 units respectively, which accounted for a 26 % and 25 % decrease with respect to vehicle group. A representative change in blood flow at 24 hours after 300 mJ/cm^2 UVB irradiation with vehicle or TAT-SOD pretreatment (300 units/cm^2 of skin area) is shown in Figure 5B. The UVB doses of 300 mJ/cm^2 was selected as equivalent to 3-MED for subject 5. The mean blood flow values in the TAT-SOD pretreated area significantly decreased from 277.0 ± 37.1 units to 189.3 ± 32.0 units compared with the vehicle pretreated area. These data suggest that TAT-SOD has a significantly suppression upon UVB induced blood flow increment. In addition, the median blood flow values measured at non-irradiated sites with vehicle and TAT-SOD pretreatment were not significantly different, indicating that there was no adverse effect on topical application of SOD mediated by HIV-TAT peptide.

Reduction on UVB-induced apoptotic sunburn cell formation by TAT-SOD

Finally, the effect of TAT-SOD pretreatment on SBC formation following UVB irradiation was investigated. SBCs, which are well known as apoptotic keratinocytes, are mainly present in the epidermis and reach a maximum density at about 24 hours after UVB irradiation [33,34]. When stained with H&E, they are easily identified morphologically with a condensed nucleus and a shrunken glassy, eosinophilic cytoplasm [35]. As previous studies reported that SBCs are absent or rare after UVA irradiation [36,37], SBC formation in the epidermis has been widely used as a biomarker of UVB induced skin damages.

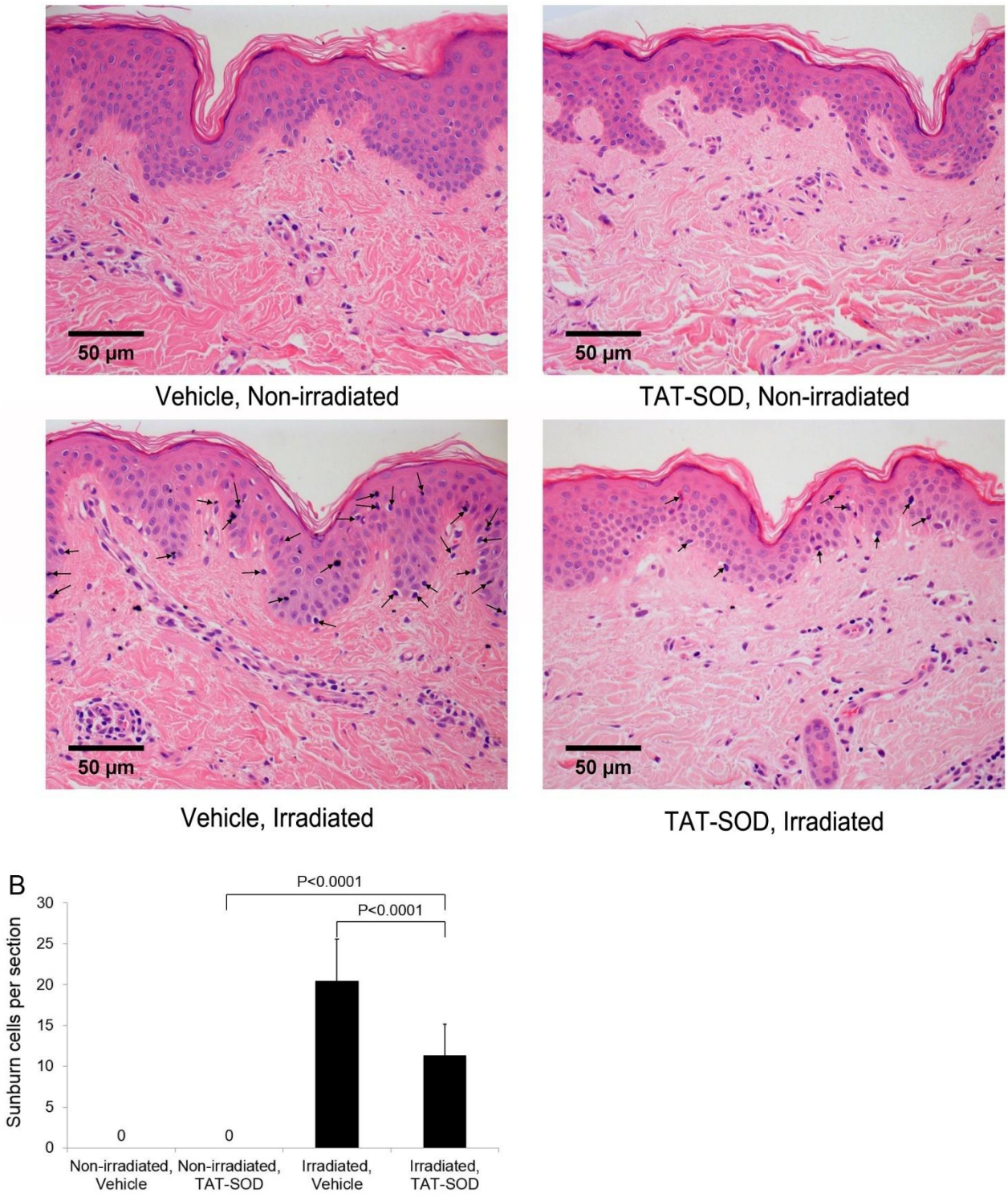

Figure 6: (A) Representative images of specimens stained for SBCs at the UVB-irradiated site and non-irradiated site (taken from subject 6). The SBC in the epidermis is indicated above the figures with an arrow. (B) The graph shows mean numbers of SBCs per section in all the test areas. Each specimen was subjected to H&E staining and photographed at a magnification of x20; scale bar = 50 µm. The number of SBCs was significantly decreased by TAT-SOD applied 1 hour before UVB

irradiation. No sunburn cells were found at the non-irradiated areas pretreated with vehicle or TAT-SOD. Data are presented as means ± SD. *P* values shown are for comparison to TAT-SOD pretreatment (n = 10, paired, two-tailed, Student's *t*-test).

Ten healthy volunteers were involved in this part of study. 24 hours after UVB irradiation, four 4mm punch biopsies were taken from 2-MED irradiated areas with TAT-SOD and vehicle pretreatment, as well as from the adjacent, non-irradiated areas with TAT-SOD and vehicle pretreatment. The amount of SBCs was quantified from paraffin-embedded sections of each skin biopsy staining with H&E and expressed as a mean number of SBCs per section. SBCs were identified in the epidermis by their shrunken eosinophilic cytoplasm and condensed nuclei.

In Figure 6A shows the epidermal localization of SBCs at 24 hours after 2-MED of UVB irradiation. Non-irradiated areas contained no SBCs, but SBCs were clearly present at 24 hours post-irradiation on irradiated area. In normalized data from all ten subjects, the mean numbers of SBCs in 2-MED of UVB irradiated areas with vehicle and TAT-SOD pretreatment were 21 ± 5 and 11 ± 4 per section respectively. Hence, the pretreatment with TAT-SOD (300 units/cm^2) 1 hour prior to 2-MED of UVB irradiation significantly reduced the apoptotic SBCs formation by 47.6 ± 8.6 % (P<0.0001). In addition, the numbers of SBCs in non-irradiated areas with vehicle or TAT-SOD pretreatment were both zero, indicating that no adverse effect was found in skin upon TAT-SOD pretreatment. These data suggest that the TAT-SOD pretreatment, 1 hour prior to UVB irradiation, significantly decreases SBC formation.

It has been realized that the importance of SBC goes far beyond that of an alternative biomarker for acute UVB injury. Numerous studies have suggested that the number of SBC which highly correlates with keratinocyte apoptosis is mainly mediated by the severity of DNA damage [38]. Two mechanisms protect against the consequences of UV-induced DNA damage. These are growth arrest followed by DNA repair and cell death by apoptosis. After a low dose of UV, most photo-lesions are removed by two major pathways of DNA repair: nucleotide excision repair and base excision repair, resulting in cell survival [39]. After a high UV dose, DNA damage will overwhelm the repair capacity of cell and cells subsequently go into programmed cell death (apoptosis). Through apoptosis, severely damaged keratinocytes will die and be eliminated as SBCs, thereby reducing the risk of further mutations which can lead to skin malignant transformation [33,34]. Accordingly, an increase of DNA repair following UV irradiation should result in a reduced ratio of SBCs. On the other hand, the reduced appearance of SBCs would indicate greater photocarcinogenic risk [40]. Indeed, there is confusion in interpreting the significance of SBCs for acute photodamage and long-term photocarcinogenesis.

Current data demonstrate that TAT-SOD plays an antiapoptotic role that we speculate indicates a reduced rather than increased susceptibility to photocarcinogenesis. The photoprotection afforded by

sunscreens produces a reduction in SBC number, consequently leading to potential protection against photocarcinogenesis [41,42]. Furthermore, several studies in mice showed that the inhibition of photocarcinogenesis is strictly associated with reduced SBC number. [43-45]. Because of only one dose of UVB (2-MED) was used to evaluate the potential effect of TAT-SOD on SBCs formation, and no marker for DNA damage was involved in the present study, the detailed mechanisms underlying these photoprotective effects of TAT-SOD are not well understood. It is not known whether TAT-SOD will increase SBC number following higher UVB doses than 2-MED, with improved regulation of DNA repair in skin. It may be that the protective effects of TAT-SOD against UVB-induced skin damages are highly UVB dose-dependent. Further studies using a wider range of UVB doses would clarify the effect TAT-SOD upon DNA damage in skin.

4. CONCLUSIONS

This is the first comparative clinical study on topical application of a permeable TAT-SOD protein against UVB-induced damage in human skin. We demonstrated that the transdermal delivery of SOD through SC was successfully achieved by mediating with HIV-TAT peptide. By replenishing the antioxidant defense of keratinocytes, TAT-SOD reduced markers of acute UVB-induced skin damage, erythema response, blood flow increment, and SBC formation. These biological effects of TAT-SOD are probably mediated via its radical scavenging properties, differentiating it from other physical sunscreen agents. Further studies are planned with the intention of evaluating whether the protective effects of TAT-SOD against UVB-induced skin damages are mediated via the inhibition of p53 gene or thymine dimer formation pathway. The mechanism by which TAT-SOD prevents UVB-induced skin damages remains to be fully elucidated as well as whether sustained application of TAT-SOD might prevent chronic UV damage over time, such as photoaging and photocarcinogenesis. In summary, the above results re-emphasize the importance of oxidative stress as an initiator of UVB-induced skin damage and also indicate that the transdermal protein/peptide delivery based on CPPs is a promising strategy to combat photodamage.

Acknowledgements

This study was jointly supported by grants from Overseas Research Scholarship from The University of Edinburgh, the Natural Science Foundation of Fujian Province (Grand No. 2015J01134) and the Natural Science Foundation of Education Department of Fujian Province (Grand No. JA15062). We thank Professor Jonathan Rees in Department of Dermatology, The University of Edinburgh for helpful discussions and reviewing the clinical research protocol. Special thanks to Mr. Craig Walker and Dr. Donald Liu in Department of Dermatology for their kind help and advice on clinical research. Thanks also go to Karen Muir and Yvonne Bisset who both play an important role in ensuring the smooth running of the study.

Conflicts of interest

None declared.

References

[1]. B.A. Gilchrest, A review of skin ageing and its medical therapy. Br. J. Dermatol. 135 (1996) 867-75.

[2]. G.J. Clydesdale, G.W. Dandie, H.K. Muller, Ultraviolet light induced injury: immunological and inflammatory effects. Immunol. Cell Biol. 79 (2001) 547-68.

[3]. F.R. de Gruijl, H.J. van Kranen, L.H. Mullenders, UV-induced DNA damage, repair, mutations and oncogenic pathways in skin cancer. J. Photochem. Photobiol. B. 63 (2001) 19-27.

[4]. K. Scharffetter-Kochanek, M. Wlaschek, P. Brenneisen, M. Schauen, R. Blaudschun, J. Wenk, UV-induced reactive oxygen species in photocarcinogenesis and photoaging. Biol. Chem. 378 (1997) 1247-57.

[5]. L. Rittie, G.J. Fisher, UV-light-induced signal cascades and skin aging. Ageing Res. Rev. 1 (2002) 705-20.

[6]. R. Scherz-Shouval, Z. Elazar, ROS, mitochondria and the regulation of autophagy. Trends Cell Biol. 17 (2007) 422-7.

[7]. Y. Shindo, E. Witt, D. Han, W. Epstein, L. Packer, Enzymic and non-enzymic antioxidants in epidermis and dermis of human skin. J. Invest. Dermatol. 102 (1994) 122-4.

[8]. Y. Shindo, T. Hashimoto, Time course of changes in antioxidant enzymes in human skin fibroblasts after UVA irradiation. J. Dermatol. Sci. 14 (1997) 225-32.

[9]. D.R. Bickers, M. Athar, Oxidative stress in the pathogenesis of skin disease. J. Invest. Dermatol. 126 (2006) 2565-75.

[10]. H. Takahashi, Y. Hashimoto, N. Aoki, M. Kinouchi, A. Ishida-Yamamoto, H. Iizuka, Copper, zinc-superoxide dismutase protects from ultraviolet B-induced apoptosis of SV40-transformed human keratinocytes: the protection is associated with the increased levels of antioxidant enzymes. J. Dermatol. Sci. 23 (2000)12-21.

[11]. D. Decraene, K. Smaers, D. Gan, T. Mammone, M. Matsui, D. Maes, L. Declercq, M. Garmyn, A synthetic superoxide dismutase/catalase mimetic (EUK-134) inhibits membrane-damage-induced activation of mitogen-activated protein kinase pathways and reduces p53 accumulation in ultraviolet B-exposed primary human keratinocytes. J. Invest. Dermatol. 122 (2004) 484-91.

[12]. K. Murakami,; J. Inagaki, M. Saito, Y. Ikeda, C. Tsuda, Y. Noda, S. Kawakami, T. Shirasawa, T. Shimizu, Skin atrophy in cytoplasmic SOD-deficient mice and its complete recovery using a vitamin C derivative. Biochem. Biophys. Res. Commun. 382 (2009)457-61.

[13]. S. Deshayes, M.C. Morris, G. Divita, F. Heitz, Cell-penetrating peptides: tools for intracellular delivery of therapeutics. Cell Mol. Life Sci. 62 (2005) 1839-49.

[14]. F. Heitz, M.C. Morris, G. Divita, Twenty years of cell-penetrating peptides: from molecular mechanisms to therapeutics. Br. J. Pharmacol. 157 (2009) 195-206.

[15]. E. Koren, V.P. Torchilin, Cell-penetrating peptides: breaking through to the other side. Trends Mol. Med. 18 (2012) 385-93.

[16]. S. A. Nasrollahi, C. Taghibiglou, E. Azizi, E. S. Farboud, Cell-penetrating peptides as a novel transdermal drug delivery system. Chem. Biol. Drug Des. 80 (2012) 639-46.

[17]. T. Uchida, T. Kanazawa, M. Kawai, Y. Takashima, H. Okada, Therapeutic effects on atopic dermatitis by anti-RelA short interfering RNA combined with functional peptides Tat and AT1002. J. Pharmacol. Exp. Ther. 338 (2011) 443-50.

[18]. A. Kashio, T. Sakamoto, A. Kakigi, M. Suzuki, K. Suzukawa, K. Kondo, et al. Topical application of the antiapoptotic TAT-FNK protein prevents aminoglycoside induced ototoxicity. Gene Ther. 19 (2012) 1141-9.

[19]. N. Ookubo, H. Michiue. M. Kitamatsu, M. Kamamura, T. Nishiki, I. Ohmori, H. Matsui, The transdermal inhibition of melanogenesis by a cell-membrane-permeable peptide delivery system based on poly-arginine. Biomaterials. 35 (2014) 4508-16.

[20]. W. Stahl, U. Heinrich, H. Jungmann, H. Sies, H. Tronnier, Carotenoids and carotenoids plus vitamin E protect against ultraviolet light-induced erythema in humans. Am. J. Clin. Nutr. 71 (2000) 795-8.

[21]. C. Herkenne, I. Alberti, A. Naik, Y. N. Kalia, F. X. Mathy, V. Préat, R. H. Guy, In vivo methods for the assessment of topical drug bioavailability. Pharm. Res. 25 (2008) 87-103.

[22]. F. Tokumura, K. Umekage, M. Sado, S. Otsuka, S. Suda, M. Taniguchi, A. Yamori, A. Nakamura, J. Kawai, K. Oka, Skin irritation due to repetitive application of adhesive tape: the influence of adhesive strength and seasonal variability. Skin Res. Technol. 11 (2005) 102-6.

[23]. M. B. Reddy, A. L. Stinchcomb, R. H. Guy, A.L. Bunge, Determining dermal absorption parameters in vivo from tape strip data. Pharm. Res. 19 (2002) 292-8.

[24]. L. K. Pershing, C. A. Reilly, J. L. Corlett, D. J. Crouch, Effects of vehicle on the uptake and elimination kinetics of capsaicinoids in human skin in vivo. Toxicol. Appl. Pharmacol. 200 (2004) 73-81.

[25]. L. Hellemans, H. Corstjens, A. Neven, L. Declercq, D. Maes, Antioxidant enzyme activity in human stratum corneum shows seasonal variation with an age-dependent recovery. J. Invest. Dermatol. 120 (2003) 434-9.

[26]. D. Redoules, R. Tarroux, M. F. Assalit, J. J. Peri, Characterisation and assay of five enzymatic activities in the stratum corneum using tape-strippings. Skin Pharmacol. Appl. Skin Physiol. 12 (1999) 182-92.

[27]. X. Chen, F. Sa'adedin, B. Deme, P. Rao, J. Bradshaw, Insertion of TAT peptide and perturbation of negatively charged model phospholipid bilayer revealed by neutron diffraction. Biochim. Biophys. Acta. 1828 (2013) 1982-8.

[28]. G. I. Harrison, A. R. Young, Ultraviolet radiation-induced erythema in human skin. Methods. 28 (2002) 14-9.

[29]. G. Murphy, A. R. Young, H. C. Wulf, D. Kulms, T. Schwarz, The molecular determinants of sunburn cell formation. Exp. Dermatol. 10 (2001) 155-60.

[30]. J. M. Sheehan, N. Cragg, C. A. Chadwick, C. S. Potten, A. R. Young, Repeated ultraviolet exposure affords the same protection against DNA photodamage and erythema in human skin types II and IV but is associated with faster DNA repair in skin type IV. J. Invest. Dermatol. 118 (2002) 825-9.

[31]. J. I. Youn, S. B. Park, B. S. Park, W. S. Han, Comparative quantitative analysis of ultraviolet B-induced skin blood flow change using laser Doppler perfusion imaging technique. Photodermatol. Photoimmunol. Photomed. 16 (2000) 167–171.

[32]. O. H. Anderson, K. Abrams, P. Bjerring, H. I. Maibach, A time correlation study of UVB induced erythema measured by reflectance spectroscopy and laser Doppler flowmetry. Photodermatol. Photoimmunol. Photomed. 8 (1991) 123–128.

[33]. J. M. Sheehan, A. R. Young, The sunburn cell revisited: an update on mechanistic aspects. Photochem. Photobiol. Sci. 1 (2002) 365-77.

[34]. S. Claerhout, A. Van Laethem, P. Agostinis, M. Garmyn, Pathways involved in sunburn cell formation: deregulation in skin cancer. Photochem. Photobiol. Sci. 5 (2006) 199-207.

[35]. F. Daniels, D. Brophy, W. C. Lobitz, Histochemical responses of human skin following ultraviolet irradiation. J. Invest. Dermatol. 37 (1961) 351-7.

[36]. I. Willis, L. Cylus, UVA erythema in skin: is it a sunburn? J. Invest. Dermatol. 68 (1977) 128-9.

[37]. R. Lavker, K. Kaidbey, The spectral dependence for UVA-induced cumulative damage in human skin. J. Invest. Dermatol. 108 (1997) 17-21.

[38]. D. Kulms, T. Schwarz, Molecular mechanisms involved in UV-induced apoptotic cell death. Skin Pharmacol. Appl. Skin Physiol. 15 (2002) 342-7.

[39]. L. Marrot, J. R. Meunier, Skin DNA photodamage and its biological consequences. J. Am. Acad. Dermatol. 58 (2008) S139-48.

[40]. T. Schwarz, A. Schwarz, DNA repair and cytokine responses. J. Investig. Dermatol. Symp. Proc. 14 (2009) 63-6.

[41]. C. A. Elmets, A. Vargas, C. Oresajo, Photoprotective effects of sunscreens in cosmetics on sunburn and Langerhans cell photodamage. Photodermatol. Photoimmunol. Photomed. 9 (1992) 113-20.

[42]. P. Wolf, C. K. Donawho, M. L. Kripke, Effect of sunscreens on UV radiation-induced enhancement of melanoma growth in mice. J. Natl. Cancer. Inst. 86 (1994) 99-105.

[43]. F. Afaq, V. M. Adhami, H. Mukhtar, Photochemoprevention of ultraviolet B signaling and photocarcinogenesis. Mutat. Res. 571 (2005) 153-73.

[44]. X. Gu, T.Wang, D. M. Collins, S. Kasichayanula, F. J. Burczynski, In vitro evaluation of concurrent use of commercially available insect repellent and sunscreen preparations. Br. J. Dermatol. 152 (2005) 1263-7.

[45]. J. Y. Lin, D. E. Fisher, Melanocyte biology and skin pigmentation. Nature. 445 (2007) 843-50.

Highlights

- Topical application of superoxide dismutase is mediated with HIV-TAT peptide.
- TAT-SOD protein efficiently penetrated through the stratum corneum.
- TAT-SOD protein significantly attenuated UVB-induced skin damage in man.

TAT-SOD or Vehicle cream pretreatment for 1 hour before UVB challenge

UVB source

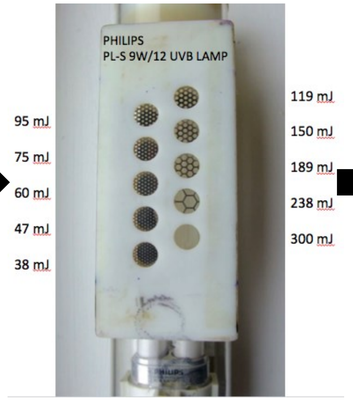

UVB challenge

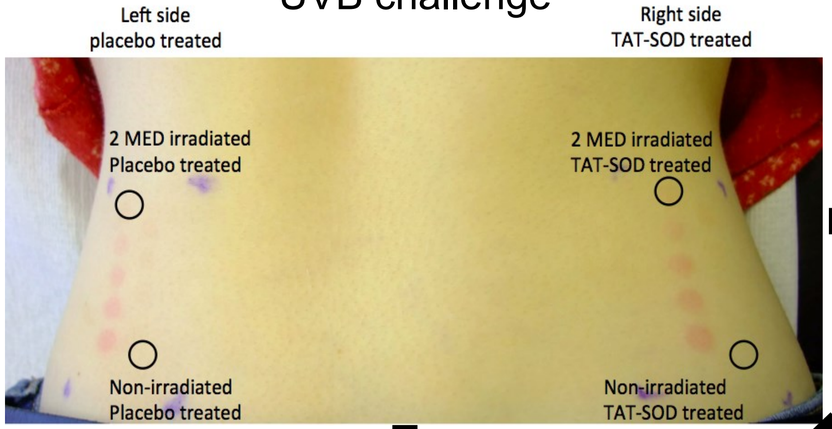

Erythema change

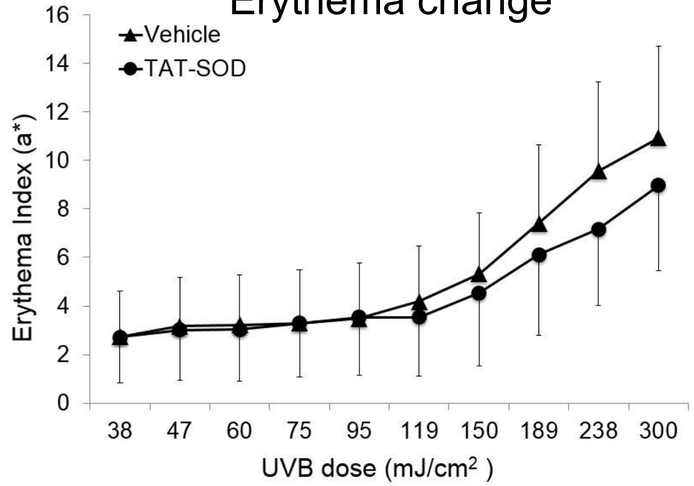

Skin biopsies for sunburn cell counting

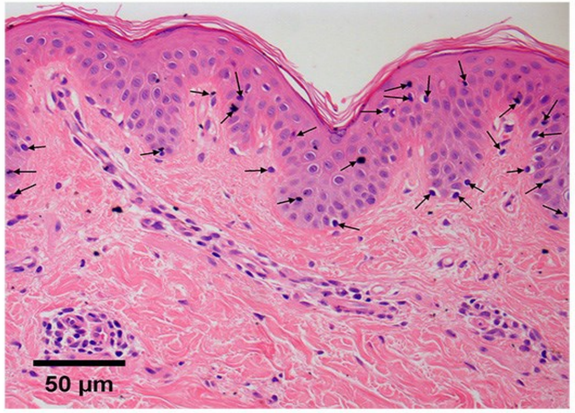

Vehicle, Irradiated

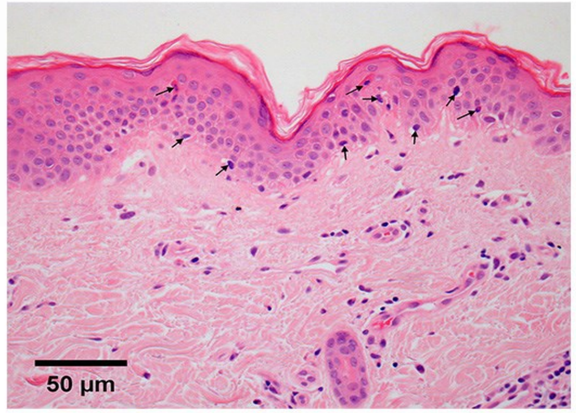

TAT-SOD, Irradiated

Blood flow change under 300 mJ/cm^2 UVB